AppliedChem

MDPI

Article

Upcycling rPET from Water Bottles into 3D-Printable Filament via Reactive Extrusion and Chain Extension

Christina Podara, Eleni Gkartzou, Christos Tsirogiannis, Theodoros Gkikarakis and Costas Charitidis *

Research Lab of Advanced, Composite, Nano Materials & Nanotechnology (R-NanoLab), School of Chemical Engineering, National Technical University of Athens, 9 Heroon Polytechniou Str., Zografos, 157 80 Athens, Greece; cpodara@chemeng.ntua.gr (C.P.); egartzou@chemeng.ntua.gr (E.G.); christsiro@chemeng.ntua.gr (C.T.)
* Correspondence: charitidis@chemeng.ntua.gr

Abstract

The recycling of polyethylene terephthalate (PET) into value-added products suitable for additive manufacturing remains challenging due to molecular degradation and insufficient melt strength. In this study, post-consumer recycled PET was upcycled via chain extension to develop filaments suitable for fused filament fabrication (FFF). Two chain extenders were evaluated: an epoxy-based multifunctional oligomer (Joncryl® ADR-4468) and a tetra-functional aromatic dianhydride (pyromellitic dianhydride, PMDA). Joncryl® ADR-4468 increased the complex viscosity and viscoelastic moduli of rPET; however, the response was non-monotonic and resulted in limited filament dimensional stability. In contrast, rPET/vPET (70/30) blends modified with PMDA exhibited a pronounced and reproducible enhancement in melt viscosity and elasticity, enabling the production of a continuous filament with a stable diameter (1.75 ± 0.05 mm). Differential scanning calorimetry indicated that PMDA had a negligible effect on the glass transition temperature, while slightly reducing crystallinity, which is beneficial for FFF processing. Preliminary printing trials confirmed stable extrusion and controlled deposition behaviour for the PMDA-modified formulation. Overall, the results demonstrate that chain extension using PMDA is an effective strategy to restore melt processability and enable the use of recycled PET in filament-based additive manufacturing.

Keywords: polyethylene terephthalate; mechanical recycling; chain extension; fused filament fabrication

1. Introduction

Polyethylene terephthalate (PET) is one of the most widely produced thermoplastic polymers of the global plastic industry (~18% of plastics), primarily used in beverage bottles, food packaging, and textiles due to its good mechanical properties, its chemical resistance, and lightweight nature [1]. The rapid and wide utilization of PET has been accompanied by a corresponding increase in PET waste, making it a significant component of the global plastic waste stream [2]. Millions of tonnes of PET waste are generated annually worldwide, with beverage bottles alone contributing a substantial share of this volume. Despite advances in recycling infrastructure, a large portion of PET continues to be landfilled or incinerated, contributing to environmental pollution and resource inefficiency [3–5].

In the European Union, the PET waste management has been significantly progressed in recent years, partly driven by regulatory targets, such as the EU Single-Use Plastics Directive [6]. According to the Independent Commodity Intelligence Services (ICIS) report

Check for updates

Academic Editor: Michael Gradzielski

Received: 15 January 2026
Revised: 31 March 2026
Accepted: 27 May 2026
Published: 3 June 2026

Copyright: © 2026 by the authors. Licensee MDPI, Basel, Switzerland. This article is an open access article distributed under the terms and conditions of the Creative Commons Attribution (CC BY) license.

for 2022, a total of approximately 5 million tons of PET (including bottles, trays, and flexible packaging) were placed on the market. From this amount, about 3 million tons were separately collected for recycling, corresponding to an overall collection rate of ~60%. Notably, PET beverage bottles constituted the vast majority of the collected materials, accounting for roughly 2.8 million tons of the total collected [7]. These numbers show that the mechanical recycling capacity in the EU is significant, reflecting optimized processing capabilities.

Despite these improvements, there are important limitations of mechanical recycling [8]. The current PET recycling is dominated by mechanical processes where the material is sorted, cleaned, shredded and then extruded into new pellet feedstock. While this is effective, this process suffers from polymer degradation and contamination, which decreases the quality and performance of the obtained material [9]. This downcycling route effectively leads PET into lower tiers of the material value chains and limits opportunities for true circularity [10].

To address this limitation, upcycling strategies have been explored to restore or even enhance polymer properties [1]. Chemical approaches, including chain extension via reactive extrusion [11] or depolymerization to monomers for repolymerization, can increase molecular weight, improve rheological behaviour, and enable high-performance applications [12,13]. Hybrid biological-chemical upcycling methods, such as enzymatic depolymerization followed by chemical functionalization, have also been investigated, demonstrating routes to produce higher-value materials from PET waste [14,15]. These strategies exemplify a shift from linear recycling to value-added circular pathways.

More specifically, to overcome the downcycling inherent to the mechanical recycling of PET, reactive extrusion with chain extenders has emerged as a promising upcycling strategy capable of restoring or enhancing polymer properties [12]. During melt reprocessing, recycled PET (rPET) undergoes chain scission and molecular weight reduction, leading to poor melt strength and inferior mechanical performance [16–18]. Chain extension counteracts these effects by reacting with terminal hydroxyl and carboxyl groups, thereby increasing molecular weight, modifying molecular architecture (linear or branched), and improving rheological behaviour [12]. As a result, chain-extended rPET exhibits enhanced melt viscosity, thermal stability, and mechanical properties, enabling its use in higher-value applications [19].

Several types of chain extenders have been successfully applied to PET. Multifunctional anhydrides such as pyromellitic dianhydride (PMDA) are widely used due to their high reactivity and ability to induce controlled branching [20]. Epoxy-functional chain extenders, including multifunctional glycidyl methacrylate-based oligomers (e.g., Joncryl®), are also extensively reported and are particularly effective under reactive extrusion conditions [21,22]. Advances in sustainable chain extender chemistry, including bio-based aromatic dianhydrides, offer routes to tailor molecular weight and thermal properties while reducing reliance on traditional extenders [23]. Additionally, the development of glycidol-free epoxy acrylate extenders provides enhanced mechanical and rheological performance without the toxicity concerns of some commercial extenders [24]. Other extenders, such as bisoxazolines and diisocyanates, have been investigated to tailor molecular weight distribution and melt behaviour, although their use requires careful control to avoid excessive crosslinking [25].

One particularly promising value-added application of rPET is Additive Manufacturing (AM), specifically Fused Filament Fabrication (FFF). PET can be valuable for AM applications due to its thermal stability, mechanical strength and chemical resistance [26]. However, mechanically recycled PET often suffers from reduced molecular weight and degraded flow properties, which limit filament quality and interlayer adhesion [27]. Recent studies have shown that upcycled PET, modified through reactive extrusion or chain exten-

sion, can produce filaments with improved melt viscosity, mechanical performance, and dimensional stability, making them suitable for FFF applications [13,28]. Such approaches not only valorize post-consumer PET but also integrate it into high-value, performance-driven manufacturing applications, bridging sustainability with material functionality.

In this context, the present study addresses key limitations associated with the use of recycled PET in FFF by systematically combining reactive extrusion, rheological–thermal characterization and printability assessment. Unlike previous studies that primarily focus on either chain extension or blend formulation, this work directly compares epoxy-based and dianhydride-based chain extenders under identical processing conditions and one-step chain extension and filament production, linking their effectiveness to filament dimensional stability and FFF processability. The influence of chain extension on melt rheology, crystallization behaviour and deposition stability is evaluated, enabling the identification of a formulation that consistently produces FFF-compatible filament. This investigation is particularly relevant considering that recycled PET feedstock originating from different post-consumer streams may exhibit significant variability in molecular weight distribution, contamination levels and thermal history. Such variability highlights the need for systematic studies that relate reactive modification strategies to process stability and performance in AM. By demonstrating the successful conversion of post-consumer PET into dimensionally stable filament using PMDA, this study provides a practical pathway for upgrading recycled PET into value-added materials suitable for AM.

2. Materials and Methods

2.1. Materials

Post-consumer polyethylene terephthalate (rPET) was obtained from locally collected water bottles. The bottles were manually sorted to remove contaminants, labels and caps, thoroughly washed, and mechanically shredded into flakes using a laboratory-scale shredder (Figure 1). Virgin PET (Lighter C93, Equipolymers, Milan, Italy) pellets were used as reference material and for blending experiments.

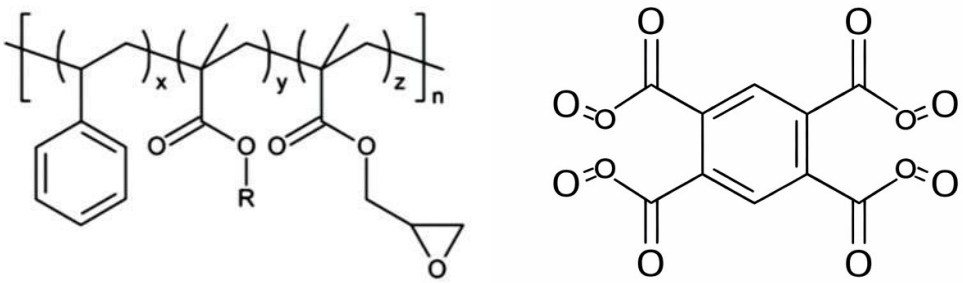

Figure 1. General chemical structure of multifunctional epoxy-based chain extender under the trade name of Joncryl® ADR-4468 (**left**) [29], and the chemical structure of pyromellitic dianhydride (PMDA) (**right**).

Two chain extenders were investigated for the chain extension process:

- Joncryl® ADR-4468 (BASF Hellas S.A., Athens, Greece), a multifunctional epoxy-based styrene–acrylic oligomer;
- Pyromellitic dianhydride or PMDA (Merck S.A. Hellas, Athens, Greece), a tetrafunctional aromatic dianhydride ($C_{10}H_2O_6$).

Their chemical structures are presented in Figure 1. In the case of Joncryl® ADR-4468, the reactivity with PET arises from the presence of the epoxy group in the oligomer. The epoxy groups undergo nucleophilic ring-opening reactions with functional end-groups of PET: carboxyl (–COOH) and hydroxyl (–OH). The reaction with carboxyl groups leads to ester linkages formation, while the reactions with hydroxyl groups lead to ether linkages.

Because the molecule contains several reactive epoxy sites, in the case of ADR-4468, it has 24 sites; a single Joncryl® ADR-4468 oligomer can react with multiple PET chains, resulting in the formation of long-chain branching structures. Under reactive extrusion conditions, this process increases the molecular weight and melt strength of the polymer while improving its rheological stability, which is particularly beneficial for the processing and upcycling of recycled PET [30].

In the case of PMDA, the reaction mechanism is different. PMDA molecule contains two highly reactive anhydride groups attached to an aromatic ring. During reactive extrusion with PET, the anhydride groups primarily react with the hydroxyl end-groups of PET chains through nucleophilic attack, causing ring opening of the anhydride functionality. This reaction forms an ester linkage between the PET chain and the dianhydride while creating one more carboxylic acid group in the PMDA. The new carboxyl group can again react with another PET hydroxyl end group, effectively linking two polymer chains through the aromatic dianhydride moiety. As a result, PMDA can link up to four PET chains, creating a 4-armed star geometry, promoting chain extension and limited branching (Figure 2), leading to an increase in molecular weight and rheology characteristics of the polymer. Due to its structure and size, it typically generates lower branching than multifunctional epoxy-based chain extenders [31].

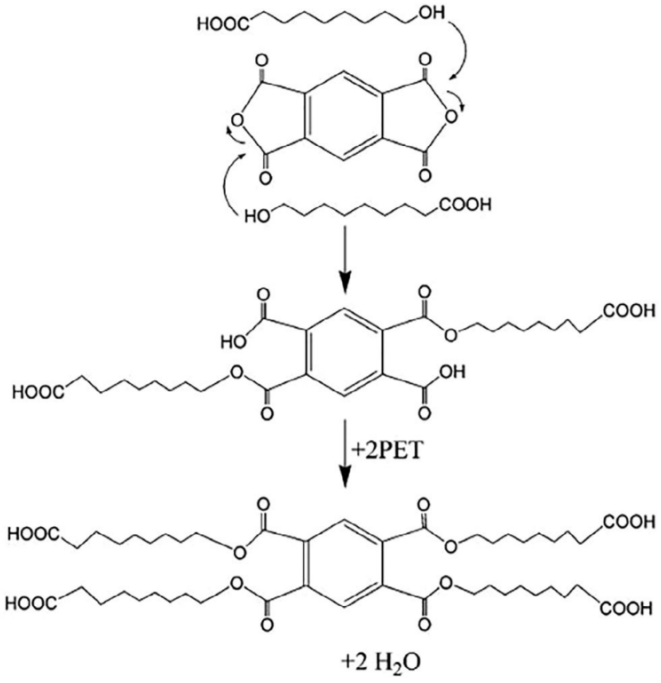

Figure 2. Reaction scheme of PMDA with PET chains. Reprinted from references [31–33].

All materials were dried prior to processing in order to minimize hydrolytic degradation. PET-based materials were dried in a convection oven at 120 °C for at least 4 h, ensuring a moisture content below 0.02 wt%.

2.2. Formulation Development for Chain Extension

Chain extension experiments were carried out by introducing the chain extenders directly into the extruder during melt processing. The equipment used for the chain extension was a laboratory-scale co-rotating twin-screw extruder (Process 11, Thermo Fisher Scientific GmbH, Karlsruhe, Germany). The extrusion temperature profile was set within the range of 245–265 °C, depending on the formulation. All prepared sample formulations and their respective nomenclatures are summarized in Table 1.

Table 1. Nomenclatures of all the developed samples.

Samples	Nomenclature
Recycled PET pellets after extrusion and pelletization of recycled PET flakes	rPET
Virgin PET pellets	vPET
Compound of recycled PET pellets and virgin PET pellets in 70/30 ratio	vPET/rPET_30/70
Compound of recycled PET and virgin PET pellets in 70/30 ratio with 0.3 wt%. PMDA chain extender	vPET/rPET_30/70_CE2_0.3
Compound of recycled PET and virgin PET pellets in 70/30 ratio with 0.6 wt%. PMDA chain extender	vPET/rPET_30/70_CE2_0.6
Compound of recycled PET pellets with 0.2 wt%. Joncryl® ADR 4468 chain extender	rPET_CE_02
Compound of recycled PET with 0.4 wt%. Joncryl® ADR 4468 chain extender	rPET_CE_04
Compound of recycled PET with 0.6 wt%. Joncryl® ADR 4468 chain extender	rPET_CE_06
Compound of recycled PET with 0.8 wt%. Joncryl® ADR 4468 chain extender	rPET_CE_08

For Joncryl® ADR-4468, rPET was compounded with additive concentrations ranging from 0.2 to 0.8 wt%. Process parameters, including screw speed, feeding rate, melt temperature and torque, were selected based on literature [22,30,34–36] and optimized to promote chain extension reactions and enhance melt strength. Specifically, the screw speed was set at 50 rpm with a starve-mode feeding rate, in order to achieve an adequate residence time (150 s) and efficient distributive mixing, enabling the reaction of PET chain ends with both Joncryl® ADR-4468 epoxy groups while minimizing thermal degradation. The extruder torque was monitored as a real-time indicator of melt viscosity increase, ensuring that chain extension occurred without inducing excessive crosslinking or machine overload. The process parameters are presented in Table 2.

Table 2. Reactive extrusion process parameters for compounds of PET with Joncryl® ADR-4468 and PMDA chain extenders.

Materials	Tm (°C)	Z1–Z8 (°C)	Screw Speed (RPM)	Residence Time (s)	Torque (%)	Vacuum
Joncryl® ADR-4468 formulations	254	170–265	50	150	60–70	Yes
PMDA formulations	264	170–270	80	120	40–50	Yes

Since Joncryl modified rPET did not yield filaments with sufficient dimensional stability, PMDA was subsequently evaluated. As the initial rPET exhibited pronounced structural degradation, leading to reduced molecular weight and unstable melt behaviour during filament extrusion, the effectiveness of PMDA-based chain extension was inherently constrained, as, unlike in the case of multifunctional epoxy-based Joncryl, polymer chains with a sufficiently long polymer backbone are required for effective melt restabilization. To address this limitation, a blend of rPET and virgin PET at a weight ratio of 70/30 was introduced, aiming to partially restore the average molecular weight and provide a more stable reactive matrix for PMDA, while maintaining a high recycled content. The addition of PMDA to the blend was conducted at concentrations of 0.3 and 0.6 wt%. Chain extension under optimized conditions, presented in Table 2, resulted in the successful production of continuous filament for the rPET/vPET (70/30) + 0.6 wt% PMDA formulation.

2.3. Preparation of PET Filament

Filament extrusion was aimed at producing a uniform filament with a nominal diameter of 1.75 ± 0.05 mm, suitable for fused filament fabrication (FFF). A melt pump and a

laser-based diameter monitoring system were used to improve dimensional stability. The extruded filament was cooled in a water bath and subsequently wound onto spools.

2.4. Rheological Characterization

Dynamic rheological measurements were carried out using a rotational rheometer (Thermo Fisher Scientific Inc., Waltham, MA, USA) (Figure 3). The rheological response of virgin PET, recycled PET, and modified formulations was evaluated by oscillatory shear measurements using a parallel-plate geometry with a plate diameter of 25 mm. The storage modulus (G′), loss modulus (G″), and complex viscosity (η*) were recorded as a function of frequency (f) over the range of 0.1–100 Hz at a testing temperature of 275 °C. Round specimens of 25 mm diameter and 1.5 mm thickness were prepared using an in-house injection moulding machine (Xplore Instruments BV, Sittard, The Netherlands).

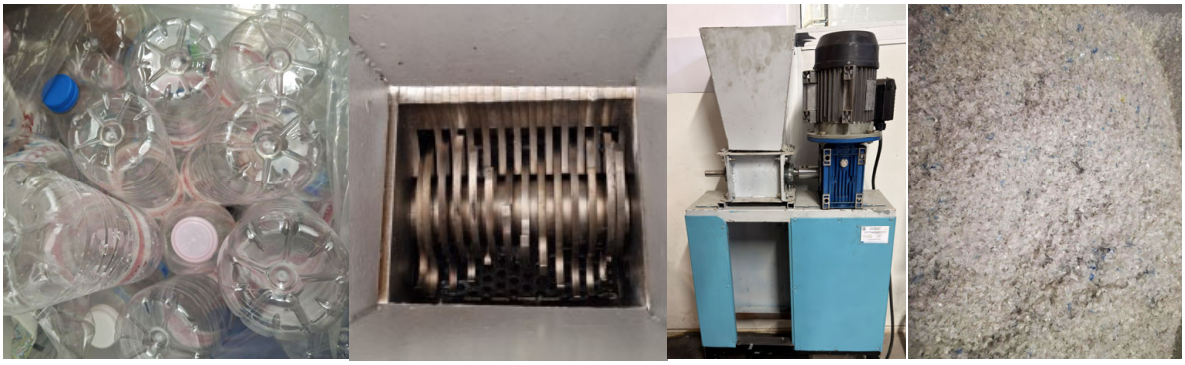

Figure 3. Shredding of collected bottles in lab-scale shredder.

2.5. Mechanical Testing

Uniaxial tensile testing was conducted using a universal testing machine (Jinan Kason Testing Equipment Co., Ltd., Jinan, China) equipped with a 5 kN load cell according to ISO 527-2 [37]. The specimens used were Type 1BA (prepared using an in-house injection moulding), and before testing, all specimens were conditioned according to ISO 291 [38], ensuring uniform temperature and humidity conditions to minimize environmental influences on the results. Testing was carried out at a constant crosshead speed of 10 mm/min. From the obtained stress–strain curves, key tensile properties were evaluated, including yield strength (σ_y, MPa), modulus of elasticity (E, Mpa), and strain at yield (ε_y, %).

2.6. Thermal Analysis

Thermogravimetric analysis (TGA) was also conducted in a TGA/DSC instrument (STA 449F5, NETZSCH-Gerätebau GmbH, Selb, Germany) with a heating rate of 50 °C/min from 25 to 850 °C under constant N_2 flow (20 mL/min). The results were used to compare degradation behaviour among virgin, recycled, and modified PET materials.

The calorimetric measurements were performed employing a TA Q200 DSC apparatus (TA Instruments, New Castle, DE, USA), calibrated with sapphires for heat capacity and indium for temperature and enthalpy, on samples of ~6–9 mg in mass, closed in TA standard aluminum pans, in the temperature range from 10 to 300 °C in a nitrogen atmosphere of high purity (99.9995%). Two measurement scans were performed, with cooling and heating rates fixed at 10 K/min.

2.7. Printability Assessment

Specimens used in this study were produced with a Prusa i3 MK3S+ FFF system (Prusa Research, Prague, Czech Republic) equipped with an E3D V6 hot end and 0.4 mm-diameter brass nozzle. Precise levelling, calibration of the FFF system, and first-layer

settings were conducted prior to each test through an induction auto-levelling sensor (SuperPINDA, Prusa Research, Prague, Czech Republic), and all specimens were printed at the same XY position to prevent levelling variability. Printing trials were conducted using varying combinations of layer height, extrusion width and printing speed. Qualitative assessment of extrudate stability, surface quality, and interlayer bonding was assessed via optical microscopy.

3. Results

3.1. Rheological Behaviour and Effect of Chain Extenders

For each polymer formulation, an initial strain sweep was performed to determine the limits of the linear viscoelastic region (LVR). Based on these measurements, a strain amplitude of 0.1% (well within the LVR) was selected and applied consistently for all subsequent frequency sweep experiments.

3.1.1. Virgin vs. Recycled

Figure 4 presents the rheological behaviour of the rPET, vPET and their blend vPET/rPET 30/70. In frequency sweep tests, as the frequency increases, the complex viscosities of all samples are decreased because of the shear-thinning behaviour of thermoplastic polymers with increasing shear rate. The most direct indicator of a polymer's stability during reprocessing is the change in its complex viscosity at the low frequency range (0.1 Hz), which is highly related to changes in the material's molecular weight, and its substantial viscosity reduction is a clear indication of chain scission [39].

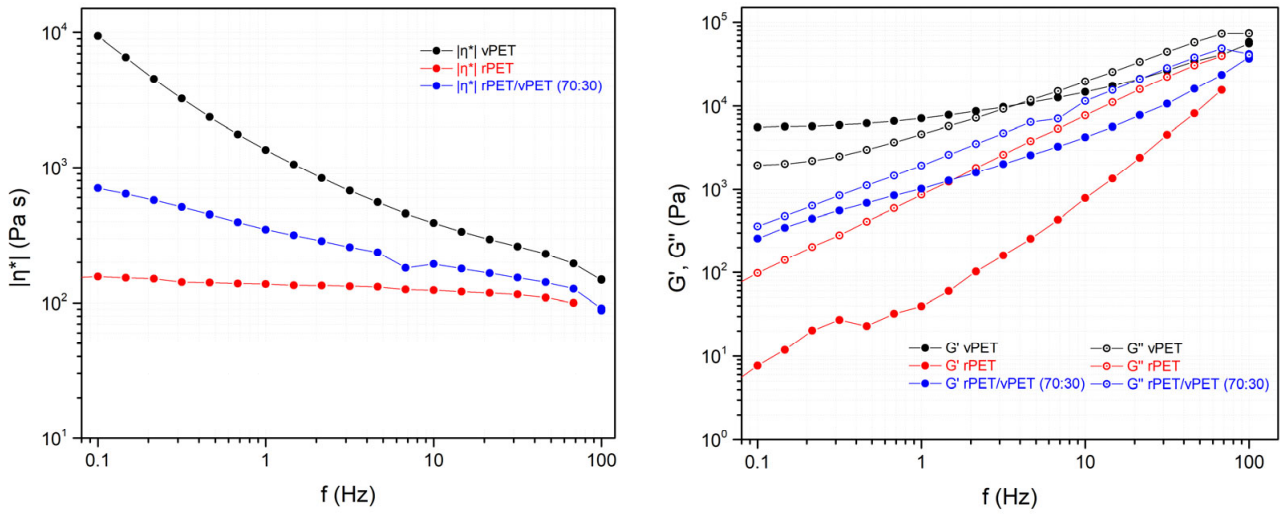

Figure 4. Complex viscosity η*, storage modulus G′, and loss modulus G″, as a function of frequency, in the range 0.1–100 Hz at 275 °C, of rPET, vPET and vPET/rPET 30/70.

As expected, unmodified recycled PET exhibited significantly lower complex viscosity compared to the virgin PET material across the entire frequency range, confirming molecular weight reduction due to thermal and hydrolytic degradation during its service life and recycling history. In both the recycled PET and the blend with virgin, the loss modulus (G″) remained higher than the storage modulus (G′) over the entire frequency range 0.1–100 Hz, indicating that the materials have predominantly viscous behaviour. The absence of a G′/G″ crossover point for rPET further indicates limited elastic response and poor melt strength, rendering it unsuitable for stable filament extrusion. The complex viscosity of the blend material is between the two as expected. Table 3 presents the complex viscosity values of virgin PET, recycled PET, and their blend, at frequencies of 0.1, 1, and 10 Hz.

Table 3. Complex viscosity (η*) values of vPET, rPET, and vPET/rPET_30/70, measured at 275 °C and frequencies of 0.1, 1, and 10 Hz. The frequency at which the storage and loss moduli intersect (G′ = G″), where observed, is also reported.

Sample	Complex Viscosity (η*) 0.1 Hz, 275 °C (Pa·s)	Complex Viscosity (η*) 1 Hz, 275 °C (Pa·s)	Complex Viscosity (η*) 10 Hz, 275 °C (Pa·s)	Cross over G′/G″
vPET	9414	1353	390.6	G′ = G″ = 10,350 Pa at f = 3.816 Hz
rPET	156.4	137.8	123.9	-
vPET/rPET_30/70	703.4	350	194.5	-

3.1.2. Joncryl® ADR-4468 Chain Extender Formulations

The formulations prepared with different concentrations of Joncryl® ADR-4468 were evaluated similarly with oscillatory frequency sweeps tests at 275 °C, in the frequency range of 0.1–100 Hz. Figure 5 presents the complex viscosities of the four formulations and the initial untreated material, as well as their storage (G′) and loss (G″) moduli, and Figure 6 presents the tan δ. Furthermore, the complex viscosity values of rPET and formulations containing different concentrations of Joncryl® ADR-4468, at frequencies of 0.1, 1, and 10 Hz, are presented graphically in Figure 7 and numerically in Table 4. The data reveal non-monotonic relationships between Joncryl® concentration and viscosity increase, which is characteristic of reactive chain extension in polyesters with epoxy-based chain extenders, due to end-group availability and cross-linking taking place [22,40].

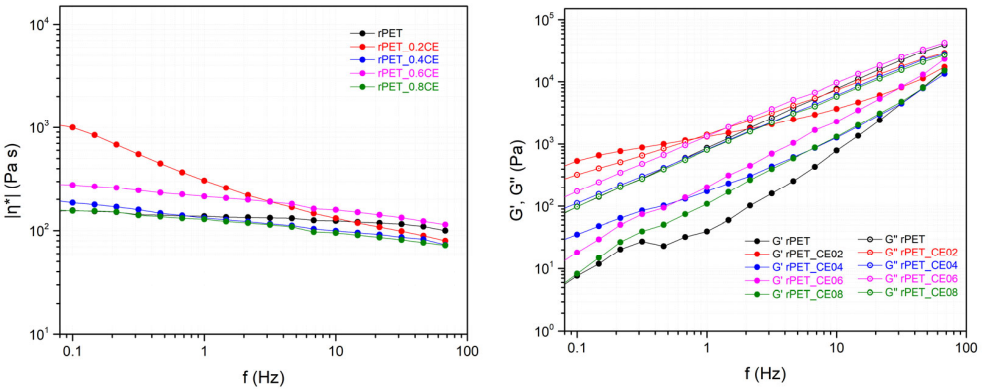

Figure 5. Comparison of complex viscosity η*, storage modulus G′, and loss modulus G″, as a function of frequency, in the range 0.1–100 Hz at 275 °C, of different formulations containing Joncryl® ADR-4468.

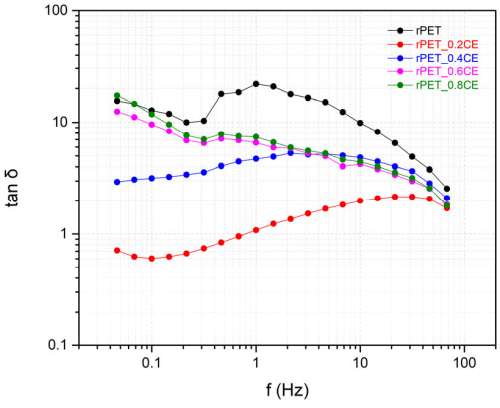

Figure 6. Comparison of tan δ, as a function of frequency, in the range 0.1–100 Hz at 275 °C, of different formulations containing Joncryl® ADR-4468.

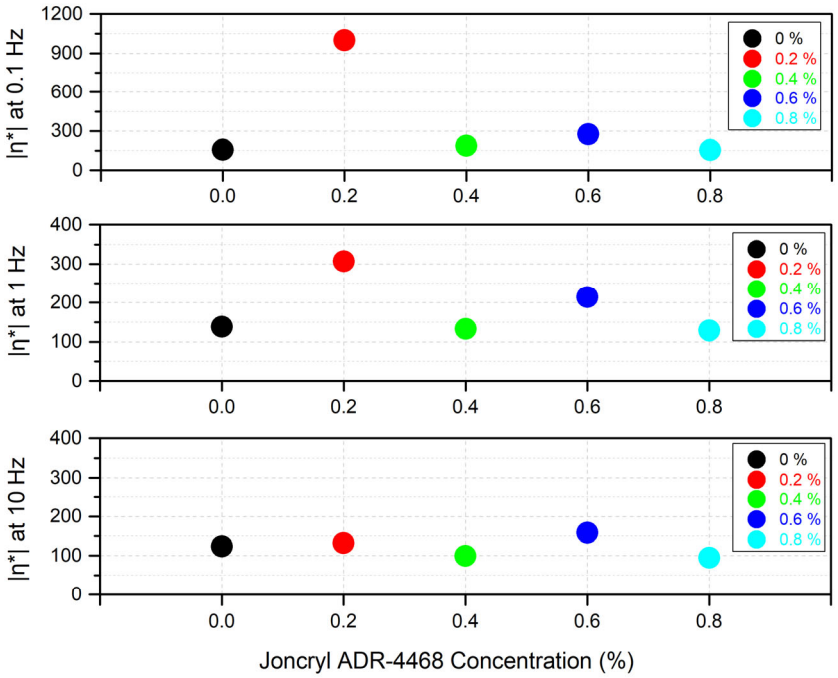

Figure 7. Complex viscosity (η*) values of rPET and rPET formulations containing different concentrations of Joncryl® ADR-4468, measured at 275 °C and frequencies of 0.1, 1, and 10 Hz.

Table 4. Complex viscosity (η*) values of rPET and rPET formulations containing different concentrations of Joncryl® ADR-4468, measured at 275 °C and frequencies of 0.1, 1, and 10 Hz. The frequency at which the storage and loss moduli intersect (G′ = G″), where observed, is also reported.

Sample	Complex Viscosity (η*) 0.1 Hz, 275 °C (Pa·s)	Complex Viscosity (η*) 1 Hz, 275 °C (Pa·s)	Complex Viscosity (η*) 10 Hz, 275 °C (Pa·s)	Cross over G′/G″
rPET	156.4	137.8	123.9	-
rPET_CE_02	998.8	306.5	131.8	G′ = G″ = 1207 Pa at f = 0.8036 Hz
rPET_CE_04	186.2	132.7	99.58	-
rPET_CE_06	276.7	213.9	158.5	-
rPET_CE_08	155.4	128.7	94.90	-

Analyzing the complex viscosity trends of Joncryl®-modified formulations, the first factor to notice is the enormous increase in the low-frequency viscosity of the rPET_02CE sample, followed by shear-thinning behaviour with a slight increase at 10 Hz, indicating the creation of high-molecular-weight polymer chains. Linear chains significantly increase low-frequency viscosity, but due to the linearity, they are easily oriented and shear-thinned at higher frequencies, hence the small change at 10 Hz. However, the fact that the storage modulus G′ is higher than the loss modulus (G″) up to a 0.8 Hz frequency indicates that long-chain branching has occurred. Based on previous studies working on Joncryl® modifications, branched polyester structures exhibit enhanced elasticity and strain hardening, with G′ dominating at low frequencies [41,42].

Regarding the other tested concentrations of the Joncryl® chain extender, the second most promising formulation is rPET_06CE. In this case, the complex viscosity was moderately increased smoothly across the whole frequency range, indicating that the molecular weight had increased, although the branching effect was not as intense as in sample rPET_02CE. Loss modulus (G″) dominated further, revealing that chain extension occurred was most probably favoured over linear extension than branched [22,40].

For the samples rPET_04CE and rPET_08CE, the results show very little complex viscosity increase, indicating that the chain extension did not occur or was limited. In the case of rPET_04CE, even though the complex viscosity is slightly increased in comparison with the initial material, there is a quite impressive increase in the storage modulus (G′), also reflected in tan δ, being the second sample after rPET_02CE to present a closer tan δ to 1. That probably indicates that the linear chain extension was favoured [22].

For the rPET_08CE sample, the results show that this concentration was excessive for the material. At concentrations exceeding the optimal stoichiometric ratio relative to available polymer end-groups, Joncryl® may not facilitate chain extension. Previous studies have demonstrated a non-linear relationship between the Joncryl® concentration and molecular weight, with concentration peaking at an optimal value and then declining at higher concentrations [43]. This may happen due to saturation of the reactive sites, leaving unreacted epoxy sites that may undergo side reactions or remain as a dispersed phase that could have a plasticizing effect, reducing the rheological properties. Similar observations have been reported in other polyester systems, where high concentrations of chain extender led to property deterioration rather than improvement [44].

Even though the enhancement of rheological properties for sample rPET_02CE seems ideal, it was insufficient for this or another sample to restore the melt elasticity required for filament dimensional stability. Consequently, continuous filament extrusion with acceptable diameter tolerance could not be achieved from these formulations.

3.1.3. PMDA Chain Extender Formulations

The PMDA chain extender was incorporated into the rPET/vPET (70/30) blend rather than the absolute waste material, as described in Section 2. In this approach, two different concentrations of PMDA were tested: one of 0.3% and one of 0.6%. Both PMDA formulations were similarly evaluated with oscillatory frequency sweeps tests at 275 °C, in the frequency range of 0.1–100 Hz. Figure 8 presents the complex viscosities of both formulations and the initial virgin/recycled PET blend, as well as their storage (G′) and loss (G″) moduli, and Figure 9 presents the tan δ. Furthermore, the complex viscosity values of virgin/recycled PET blend and PMDA formulations at frequencies of 0.1, 1, and 10 Hz are presented graphically in Figure 10 and numerically in Table 5.

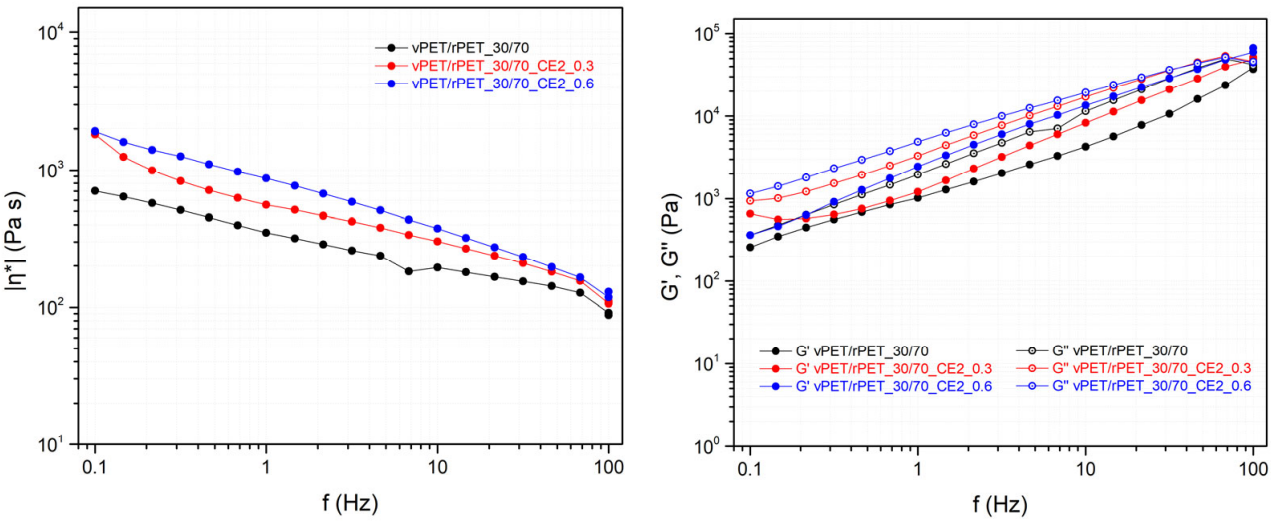

Figure 8. Comparison of complex viscosity η*, storage modulus G′, and loss modulus G″, as a function of frequency, in the range 0.1–100 Hz at 275 °C, of different formulations containing PMDA chain extender.

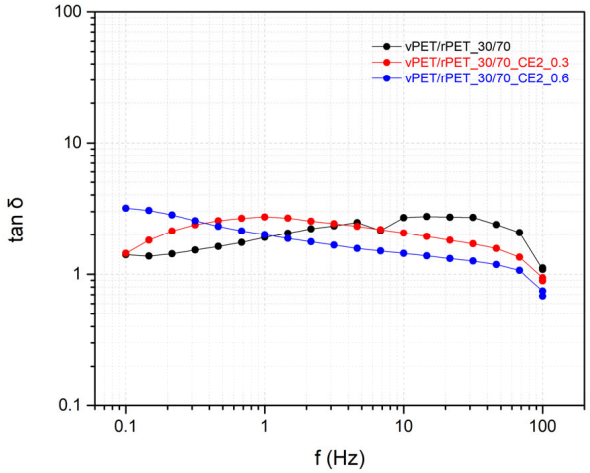

Figure 9. Comparison of tan δ, as a function of frequency, in the range 0.1–100 Hz at 275 °C, of different formulations containing PMDA chain extender.

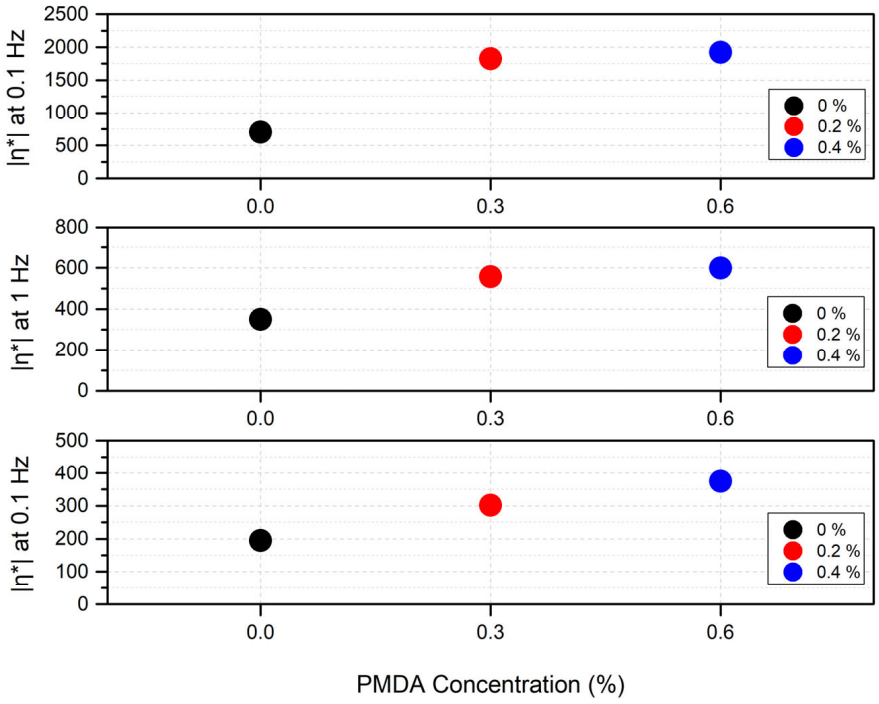

Figure 10. Complex viscosity (η*) values of vPET/rPET_70/30 and the formulations containing different concentrations of PMDA, measured at 275 °C and frequencies of 0.1, 1, and 10 Hz.

Table 5. Complex viscosity (η*) values of rPET, vPET, blend, and formulations containing different concentrations of PMDA, measured at 275 °C and frequencies of 0.1, 1, and 10 Hz. The frequency at which the storage and loss moduli intersect (G′ = G″), where observed, is also reported.

Sample	Complex Viscosity (η*) 0.1 Hz, 275 °C (Pa·s)	Complex Viscosity (η*) 1 Hz, 275 °C (Pa·s)	Complex Viscosity (η*) 10 Hz, 275 °C (Pa·s)	Cross over G′/G″
rPET	156.4	137.8	123.9	-
vPET	9414	1353	390.6	G′ = G″ = 10350 Pa at@ f = 3.816 Hz
vPET/rPET_30/70	703.4	350	194.5	-
vPET/rPET_30/70_CE2_0.3	1824	556.8	301.9	-
vPET/rPET_30/70_CE2_0.6	1922	598.3	375	-

In this case, the addition of PMDA led to an increased complex viscosity for both concentrations, particularly at low frequencies, while maintaining similar shear-thinning

behaviour for both chain extender concentrations. These trends indicate that PMDA effectively reacted with the PET chains, resulting in an increased molecular weight, mostly by linear extension and limited branching. This was expected since the PMDA chain extender has four reactive sites.

The formulation containing 0.6 wt% PMDA exhibited the highest viscosity values and stable rheological behaviour, enabling one-step reactive extrusion and consistent filament production within the target diameter range (1.75 ± 0.05 mm). This improvement is attributed to the higher reactivity of PMDA toward PET end groups, promoting more effective chain extension and branching compared to the epoxy-based modifier.

3.2. Thermal Properties

Thermal stability was assessed using thermogravimetric analysis (TGA). All materials exhibited similar degradation profiles, as shown in Figure 11, with no significant shifts in degradation onset temperature or decomposition mechanism following chain extension. This indicates that neither Joncryl® ADR-4468 nor PMDA adversely affected the thermal stability of PET.

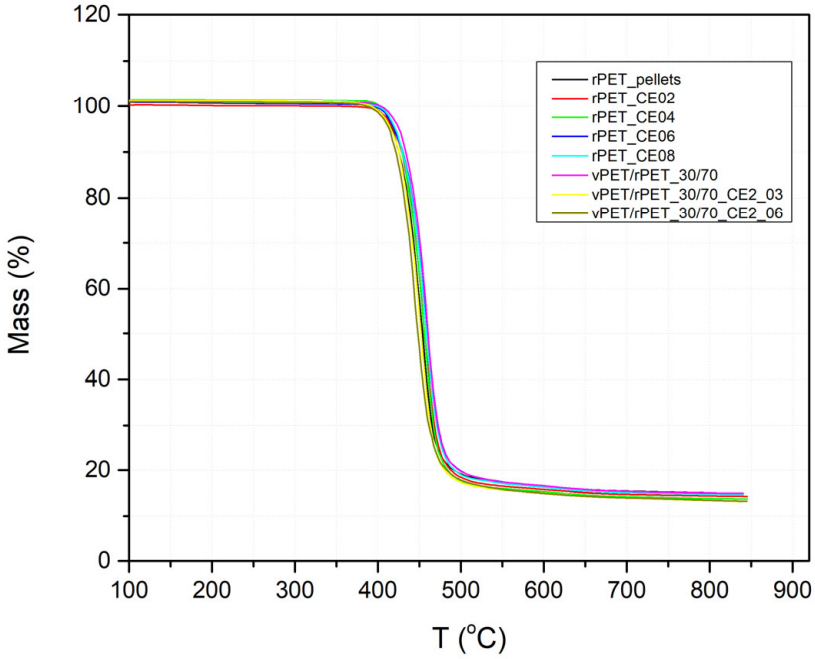

Figure 11. TGA thermograms for all PET formulations (25–850 °C, 20.0 °C/min).

DSC was employed to evaluate the thermal behaviour of vPET, rPET, their blends, and PMDA-modified formulations, as these were the most promising ones. The thermal parameters reported in this study were derived from the second heating cycle in order to eliminate the influence of prior thermal history arising from processing and sample preparation, thereby allowing a consistent comparison of the intrinsic thermal behaviour of the investigated PET formulations [45,46].

Table 6 presents the thermal properties results obtained from the second heating cycle of vPET, rPET, their blend, and blends containing 0.3 wt% and 0.6 wt% PMDA. Respective thermograms are presented in Figure 12.

Specifically, the reported results include the crystallization temperature (Tc), crystallization enthalpy (ΔHc), glass transition temperature (Tg), cold crystallization temperature (Tcc), cold crystallization enthalpy (ΔHcc), melting enthalpy (ΔHm), and degree of crystallinity (Xc). The degree of crystallinity was calculated by dividing the measured melting enthalpy by the theoretical melting enthalpy of 100% crystalline PET, taken as 140 J g^{-1}.

Table 6. Thermal properties obtained during the second DSC heating scan for vPET, rPET, rPET/vPET_70/30, and PMDA-modified formulations.

	Cooling		Heating					
	T_c (°C)	ΔH_c (J/g)	T_g (°C)	T_{cc} (°C)	ΔH_{cc} (J/g)	T_m (°C)	ΔH_m (J/g)	X_c (%)
vPET	187.1	−36.9	80.7	165.1	−2.50	253.5	36.4	26.0
rPET/vPET_70/30	202.3	−40.0	80.6	-	-	244.0/250.5	37.8	27.0
rPET	202.8	−37.4	81.5	-	-	244.4	33.0	23.5
rPET/vPET_70/30_CE2_03	198.2	−41.7	81.4	-	-	241.1/247.8	34.4	24.6
rPET/vPET_70/30_CE2_06	195.5	−38.7	81.9	-	-	240.8/246.7	30.2	21.6

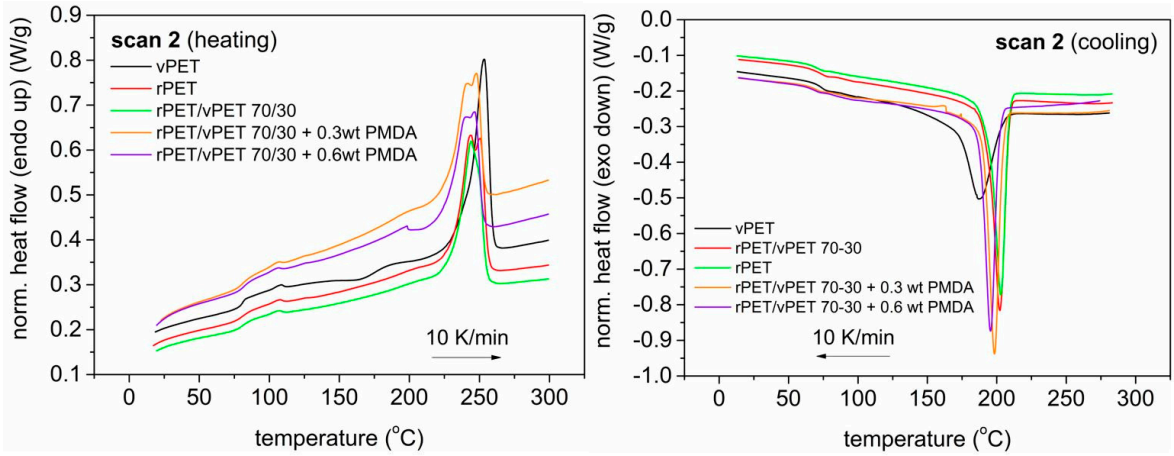

Figure 12. DSC thermograms obtained during the second heating (**left**) and cooling (**right**) scan for vPET, rPET, rPET/vPET_70/30, and PMDA-modified formulations. Measurements were performed at a heating rate of 10 K/min.

The glass transition temperature (Tg) showed only minor variations among the examined materials. Although PMDA is known to introduce chain extension and branching, which could theoretically restrict chain mobility and increase Tg, the experimental results indicate that Tg remains largely unaffected by the addition of PMDA. A very slight increase in Tg was observed for rPET/vPET blends with increasing PMDA concentrations; however, this change was minimal and does not allow for definitive conclusions regarding the influence of PMDA on the glass transition behaviour.

Significant differences were observed in the crystallization behaviour of the materials. Cold crystallization was detected only in vPET, indicating that vPET requires higher cooling rates than rPET to suppress crystallization and retain an amorphous structure. In addition, vPET exhibited a lower crystallization temperature and a broader crystallization peak compared to rPET. In contrast, rPET displayed faster crystallization kinetics, which can be attributed to its shorter polymer chains and the presence of residual impurities that may act as nucleating agents, thereby promoting crystal formation more readily than in the more structurally uniform vPET.

Regarding melting behaviour, vPET exhibited a sharper melting peak, consistent with its higher purity and more homogeneous crystalline structure. rPET-containing samples reached their melting temperature at approximately 244 °C, reflecting partial degradation of thermal properties caused by thermo-mechanical stress and molecular weight reduction during recycling. A double melting peak was observed for rPET/vPET_70/30, both with and without PMDA. This phenomenon is commonly associated with the melting of primary and secondary crystalline populations (lamellae) with different thickness distributions formed during crystallization. Additionally, all materials exhibited a minor thermal event

at approximately 106 °C, which may be associated with physical ageing effects or the melting of imperfect or secondary crystalline regions.

Finally, a reduction in the degree of crystallinity was observed for rPET/vPET_70/30 blends containing PMDA. More specifically, the degree of crystallinity was reduced by 2.4% in the rPET/vPET_70/30 CE2_03 sample, while in the case of rPET/vPET_70/30_CE2_06, the reduction was 5.4%. A reduction of up to 5% in the degree of crystallinity can be considered important for PET systems, as relatively small variations in crystallinity are known to influence crystallization kinetics, molecular mobility, and mechanical performance in semi-crystalline polymers. Previous studies have reported that crystallinity changes of a few percent are sufficient to alter the structural and mechanical behaviour of PET during processing [47,48]. This decrease in crystallinity is considered advantageous for processing via fused filament fabrication (FFF), as it may limit excessive crystallization during cooling and promote improved interlayer adhesion.

3.3. Mechanical Properties

The tensile properties of all formulations were evaluated to assess the impact of chain extension on mechanical performance. Table 7 summarizes the tensile strength, elongation at break, and modulus of elasticity. Figure 13 presents a comparison of the tensile strength, strain at break, and modulus of elasticity of the tested rPET, vPET, rPET/vPET blend, and the most promising formulations of both chain-extenders, which are the rPET_CE_02 and the rPET_CE_06 in the case of Joncryl® ADR-4468 and the vPET/rPET_ 30/70_CE2_0.3 and vPET/rPET_30/70_CE2_0.6 in the case of the PMDA chain extender. Since most of the results fall in the range of standard deviations, one-way ANOVA analysis was performed to reveal if there is statistical significance in these results.

Table 7. Tensile strength, strain at break, and modulus of elasticity of rPET, vPET, and rPET/vPET blends, and most promising chain-extended formulations. Values are reported as mean ± standard deviation.

Samples	Tensile Strength (MPa)	Strain at Break (%)	Modulus of Elasticity (MPa)
rPET	56.91 ± 2.64	25.31 ± 2.92	1934 ± 55
vPET	57.40 ± 2.00	15.18 ± 7.02	2029 ± 75
vPET/rPET_30/70	58.01 ± 0.55	23.57 ± 2.57	2001 ± 14
vPET/rPET_30/70_CE2_0.3	57.50 ± 1.49	23.21 ± 2.04	2010 ± 17
vPET/rPET_30/70_CE2_0.6	60.15 ± 2.00	23.23 ± 4.37	2204 ± 61
rPET_CE_02	57.59 ± 0.24	24.05 ± 3.85	1922 ± 34
rPET_CE_06	57.41 ± 2.14	21.27 ± 0.89	1973 ± 83

Tensile strength values of all different samples vary between 56.9 and 60.2 MPa; sample vPET/rPET_30/70_CE2_0.6 exhibited a slightly higher value (60.15 MPa), although the statistical analysis revealed that differences among the formulations were not statistically significant ($F(6, 28) = 1.79$, $p = 0.138$). The strain at break values exhibited even larger variability, ranging from approximately 15% to 25%. In this case, the ANOVA analysis yielded $F(6, 28) = 2.31$ with $p = 0.062$, which is slightly above the commonly used significance threshold of 0.05. Consequently, the differences cannot be considered statistically significant. The relatively large overlap between the standard deviation ranges of the samples suggests that the observed variations fall within experimental scatter.

In contrast, the elastic modulus showed statistically significant differences among the formulations. The measured values ranged from approximately 1920 MPa to 2204 MPa, with the vPET/rPET_30/70_CE2_0.6 sample exhibiting a clearly higher stiffness (2204 ± 61 MPa). The ANOVA analysis confirmed the statistical significance of this variation ($F(6, 28) = 11.06$, $p < 0.001$). The increased stiffness of the vPET/rPET_30/70_CE2_0.6 sample can be attributed to chain extension, partial branching, or the differences in crys-

talline morphology. Such structural modifications can restrict chain mobility and increase resistance to elastic deformation, resulting in higher stiffness.

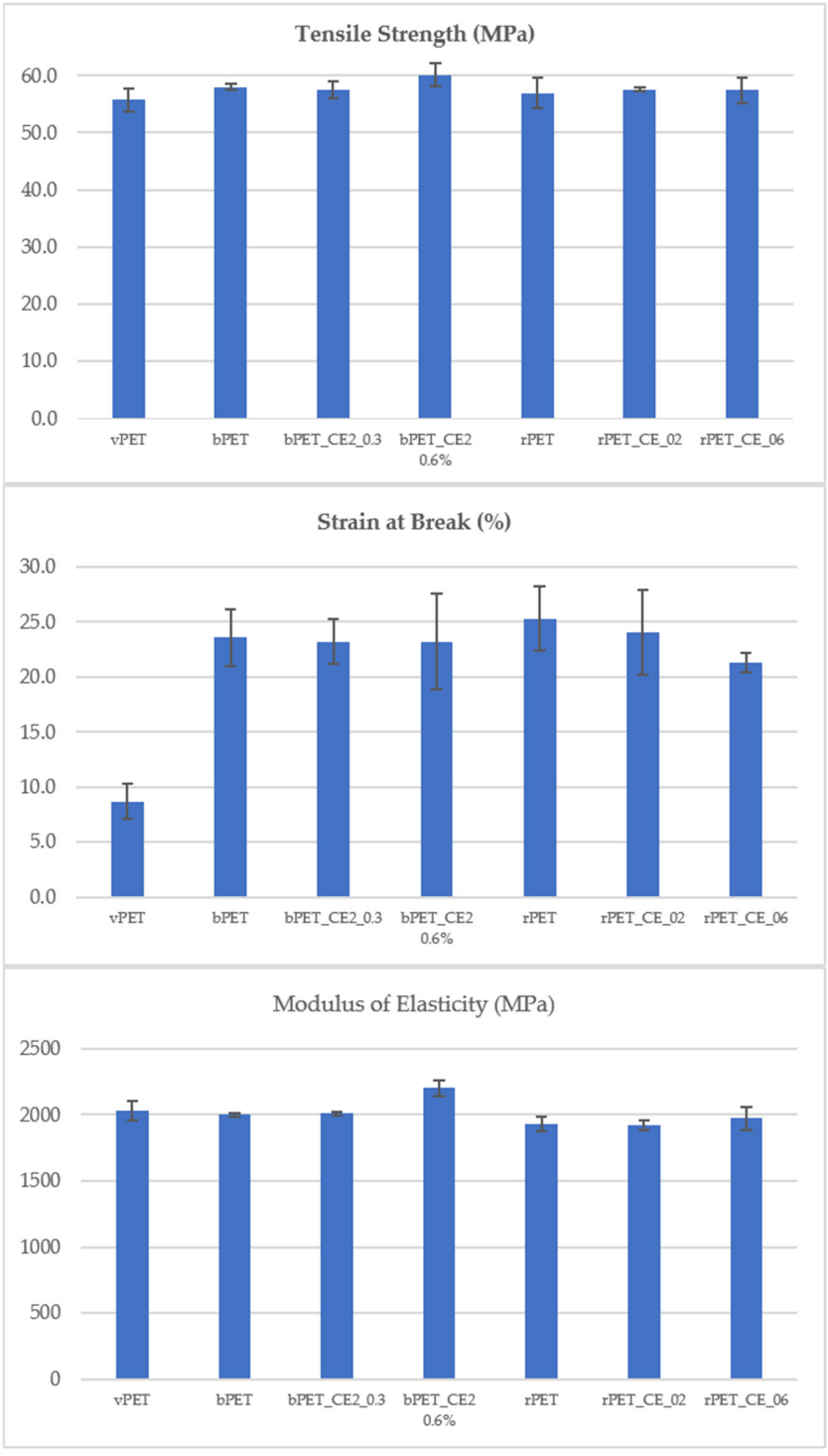

Figure 13. Tensile Strength, strain at break, and modulus of elasticity of rPET, vPET, and rPET/vPET blends, and chain-extended formulations.

This result indicates that the incorporation of the investigated formulations did not substantially affect the ultimate tensile strength and strain at break of PET. Similar observations have been reported in the literature for chain-extended PET systems, where chain-extension reactions primarily modify the molecular architecture by increasing molecular weight and introducing branching, leading to significant changes in melt rheology.

However, the tensile properties of semi-crystalline polymers such as PET are predominantly governed by the solid-state microstructure, including the degree of crystallinity, crystal size and distribution, and the properties of the amorphous phase. Since the DSC analysis did not reveal significant variations in crystallinity among the investigated formulations, except for the case of the vPET/rPET_30/70_CE2_0.6 formulation, the overall microstructure of the other formulations remains relatively unaffected, resulting in comparable tensile behaviour [49,50].

3.4. Filament Stability and Printability

A preliminary assessment of printability was conducted for the rPET/vPET (70/30) blend containing 0.6 wt% PMDA, which had previously demonstrated stable filament diameter within the targeted range. Specimens were fabricated using a Prusa i3 MK3S+ fused filament fabrication (FFF) 3D printer equipped with an E3D V6 hotend and a hardened steel nozzle with a diameter of 0.6 mm. Prior to each printing trial, careful system levelling and first-layer calibration were performed, and all specimens were printed at the same XY position to minimize positional variability.

To qualitatively assess material flow through the nozzle, extrusion behaviour was initially evaluated at different printing temperatures. A stable and continuous extrusion was achieved at a nozzle temperature of 270 °C, which was therefore selected for subsequent printing trials. The extrusion width was set to 1.2 times the nozzle diameter, corresponding to 0.72 mm, in accordance with standard FFF practice. Two-layer heights (0.3 and 0.4 mm) and three printing speeds (20, 40, and 60 mm s^{-1}) were investigated, while all other processing parameters were kept constant. A double-sided textured PEI-coated spring steel sheet was used as the build surface, and the bed temperature was maintained at 100 °C to promote adhesion.

As shown in Figure 14, the specimens consisted of single-filament stacks arranged in a uniform pattern and grouped into three printing-speed zones for each layer height. The effect of printing parameters on filament deposition stability was evaluated in terms of dimensional accuracy and surface morphology. Qualitative inspection of the top surface was performed using a digital microscope (Emspira 3, Leica Microsystems GmbH, Wetzlar, Germany).

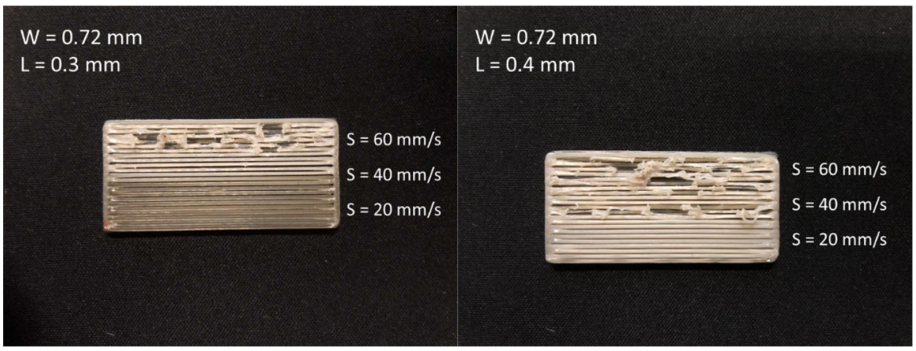

Figure 14. Indicative images of the samples produced for the printability evaluation. Each sample has 3 print speed zones for each combination of W and L.

Based on visual assessment, the most promising printing parameter set was identified as a layer height of 0.3 mm, extrusion width of 0.72 mm, and printing speed of 20 mm s^{-1}.

Under these conditions, the deposited filaments retained optical transparency, indicating a predominantly amorphous morphology. In the amorphous state, polymeric chains are randomly arranged, resulting in a relatively homogeneous material with a uniform refractive index and minimal light scattering, which allows light to pass through the material. In contrast, all other parameter combinations resulted in opaque filaments with reduced light

transmittance, suggesting increased crystallinity. This behaviour can be attributed to the formation of crystalline regions (spherulites), which introduce refractive index heterogeneities between the crystalline and amorphous phases. These heterogeneities act as scattering centres, particularly when the size of the crystalline structures is comparable to the wavelength of visible light, leading to significant light scattering and loss of transparency. Therefore, the observed optical appearance provides qualitative evidence of differences in the degree of crystallinity and microstructural organization of the filaments [51].

These observations suggest a direct relationship between printing parameters and crystallization kinetics. Increased volumetric flow rate, resulting from higher printing speed or higher layer height, leads to higher shear stresses during extrusion and increased material volume, both of which can promote crystallization. In semicrystalline polymer systems, shear and extensional stresses during FFF extrusion can induce partial alignment of polymer chains along the flow direction, thereby promoting strain-induced crystallization [52]. In parallel, the deposition of larger material volumes increases the thermal mass of the extruded bead and prolongs cooling times, allowing greater molecular mobility during solidification. Consequently, the combined effect of these phenomena and associated FFF parameter combinations may either suppress or favour crystallization, thereby influencing the final properties of FFF-printed parts. These results suggest that the investigated rPET blend is highly sensitive to variations in processing conditions, which can lead to significant changes in its structural evolution during printing.

Additional parameter sets (L = 0.3 mm, W = 0.72 mm, S = 40 mm s^{-1} and L = 0.4 mm, W = 0.72 mm, S = 20 mm s^{-1}) also produced continuous extrudate deposition, albeit with higher opacity. These configurations were further examined at higher magnification to analyze filament cross-sections obtained by vertical sectioning of the specimens (Tables 8–10).

Table 8. Indicative images of the morphology of the filaments obtained from different combinations of FFF process parameters (scale equals 1 mm).

	Layer Height = 0.3 mm	**Layer Height = 0.4 mm**
Printing speed = 20 mm/s		
Printing speed = 40 mm/s	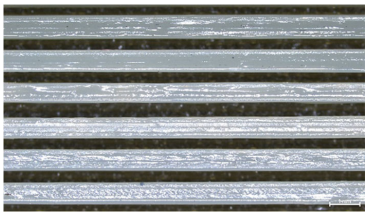	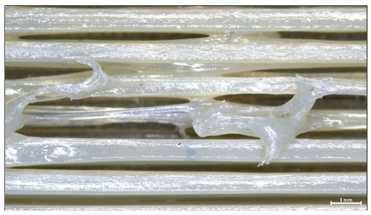
Printing speed = 60 mm/s		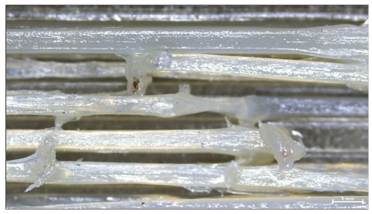

Table 9. Further inspection of the top surface and the sliced cross-section of the most promising printing parameter sets (scale line equal to 750 µm).

	Layer Height = 0.3 mm	
	Top Surface	**Sliced Cross-Section**
Printing speed = 20 mm/s	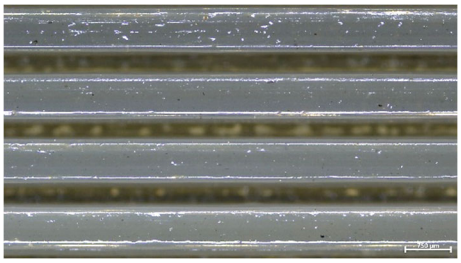	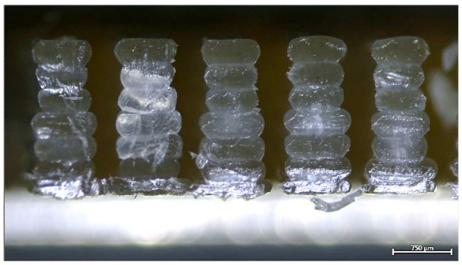
Printing speed = 40 mm/s	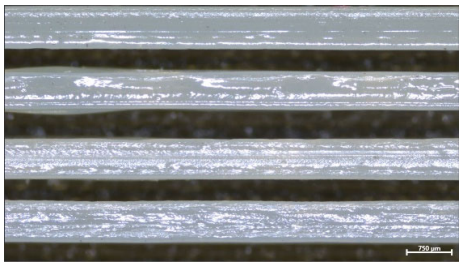	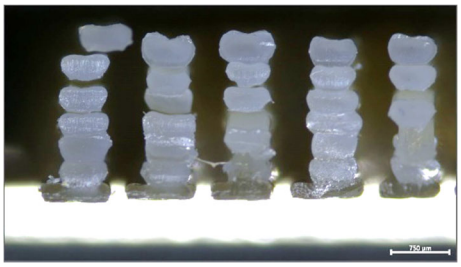
	Layer height = 0.4 mm	
	Top surface	Sliced cross-section
Printing speed = 20 mm/s	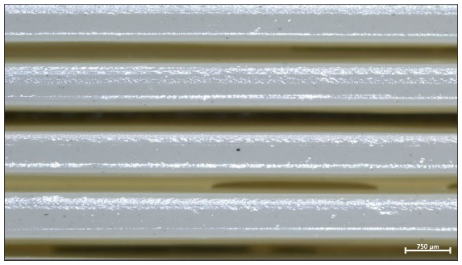	

Table 10. Mean diameter and standard deviation values for the most promising printing parameters in vertical sections.

Layer Height = 0.3 mm		
Printing speed (mm/s)	Mean diameter (mm)	Standard deviation (mm)
20	0.7272	0.0700
40	0.6121	0.0470
Layer Height = 0.4 mm		
	Mean diameter (mm)	Standard deviation (mm)
20	0.8457	0.0636

4. Conclusions

In this work, recycled PET was successfully processed into FFF-compatible filament through reactive extrusion and formulation optimization. The influence of two different chain extenders on the rheological, thermal, and processing behaviour of rPET-based formulations was evaluated.

The use of Joncryl® ADR-4468 resulted in partial enhancement of rheological properties; however, the non-uniform response and limited filament dimensional stability highlighted the sensitivity of epoxy-based chain extension to processing conditions and residence time. In contrast, PMDA proved to be a highly effective chain extender when

combined with a 70/30 rPET/vPET blend, providing reproducible increases in complex viscosity and melt elasticity that enabled stable filament extrusion.

Thermal analysis showed that PMDA had a minimal impact on the glass transition temperature, while inducing a slight reduction in crystallinity. This reduction was found to be advantageous for FFF processing, as it limited excessive crystallization during cooling and promoted improved filament deposition behaviour. Preliminary printing trials confirmed that optimized combinations of layer height, extrusion width, and printing speed significantly influenced crystallization kinetics and filament morphology, with lower volumetric flow rates favouring transparent, low-crystallinity deposits.

Overall, the findings demonstrate that chain extension with PMDA is a promising approach for upgrading recycled PET into high-value filaments suitable for additive manufacturing. The proposed strategy contributes to the sustainable utilization of post-consumer PET and provides a framework for further optimization of recycled polymer systems for FFF applications.

Author Contributions: Conceptualization, C.P. and E.G.; methodology, C.P., E.G., C.T. and T.G.; writing—original draft preparation, C.P.; writing—review and editing, C.P. and E.G.; visualization, C.P., E.G. and C.T.; supervision, C.C. All authors have read and agreed to the published version of the manuscript.

Funding: This research received no external funding.

Institutional Review Board Statement: Not applicable.

Informed Consent Statement: Not applicable.

Data Availability Statement: The raw data supporting the conclusions of this article will be made available by the authors on request.

Acknowledgments: The authors thank the Dielectrics Research Group of the School of Applied Mathematical and Physical Sciences of the National Technical University of Athens, and specifically Panagiotis Klonos, for his assistance with differential scanning calorimetry (DSC) measurements.

Conflicts of Interest: The authors declare no conflicts of interest.

References

1. Istirokhatun, T.; Siahaan, S.E.; Susanto, H.; Gonzales, R.R.; Filardli, A.M.I.; Andarani, P.; Matsuyama, H. Novel Methods for Recycling PET Plastic Bottle Waste: Progressing Membrane Engineering Using Environmentally Friendly Solutions. *J. Clean. Prod.* **2025**, *532*, 146967. [CrossRef]
2. Duan, C.; Wang, Z.; Zhou, B.; Yao, X. Global Polyethylene Terephthalate (PET) Plastic Supply Chain Resource Metabolism Efficiency and Carbon Emissions Co-Reduction Strategies. *Sustainability* **2024**, *16*, 3926. [CrossRef]
3. Benyathiar, P.; Kumar, P.; Carpenter, G.; Brace, J.; Mishra, D.K. Polyethylene Terephthalate (PET) Bottle-to-Bottle Recycling for the Beverage Industry: A Review. *Polymers* **2022**, *14*, 2366. [CrossRef] [PubMed]
4. Ren, T.; Zhan, H.; Xu, H.; Chen, L.; Shen, W.; Xu, Y.; Zhao, D.; Shao, Y.; Wang, Y. Recycling and High-Value Utilization of Polyethylene Terephthalate Wastes: A Review. *Environ. Res.* **2024**, *249*, 118428. [CrossRef]
5. Guo, Z.; Wu, J.; Wang, J. Chemical Degradation and Recycling of Polyethylene Terephthalate (PET): A Review. *RSC Sustain.* **2025**, *3*, 2111–2133. [CrossRef]
6. European Union. Directive (EU) 2019/904 of the European Parliament and of the Council of 5 June 2019 on the reduction of the impact of certain plastic products on the environment. *Off. J. Eur. Union L* **2019**, *155*, 1–19. Available online: https://eur-lex.europa.eu/eli/dir/2019/904/oj (accessed on 8 January 2026).
7. ICIS. PET Market in Europe—State of Play: Production, Collection & Recycling Data 2022. Produced in Partnership with PETCORE Europe, UNESDA Soft Drinks Europe, Plastics Recyclers Europe, and Natural Mineral Waters Europe. 2022. Available online: https://unesda.eu/wp-content/uploads/2024/05/PET-plastic-Market-in-Europe-State-of-Play-Production-Collection-Recycling-Data_2022.pdf (accessed on 8 January 2026).
8. Klotz, M.; Haupt, M.; Hellweg, S. Potentials and Limits of Mechanical Plastic Recycling. *J. Ind. Ecol.* **2023**, *27*, 1043–1059. [CrossRef]

9. Damayanti, D.; Marpaung, D.S.S.; Kodarif, A.R.; Sanjaya, A.; Saputri, D.R.; Fahni, Y.; Rahmiyati, L.; Silvia, P.Z.; A'yuni, D.Q.; Imalia, C.L.; et al. Biocatalytic Recycling of Polyethylene Terephthalate: From Conventional to Innovative Routes for Transforming Plastic and Textile Waste into Renewable Resources. *Resources* **2025**, *14*, 176. [CrossRef]
10. Han, J.; Zuo, J.; Zillante, G.; Chang, R.; Du, L. A Systematic Review of PET Circularity Technologies and Management Strategies: Challenges and Future Directions. *Resour. Conserv. Recycl.* **2025**, *219*, 108280. [CrossRef]
11. Jang, J.Y.; Sadeghi, K.; Seo, J. Chain-Extending Modification for Value-Added Recycled PET: A Review. *Polym. Rev.* **2022**, *62*, 860–889. [CrossRef]
12. Galan, N.J.; Dishner, I.T.; Sumpter, B.G.; Kertesz, V.; Abdul Rahman, N.B.; Polo-Garzon, F.; Demchuk, Z.; Saito, T.; Foster, J.C. Upcycling of Polyethylene Terephthalate to High-Value Chemicals by Carbonate-Interchange Deconstruction. *Green. Chem.* **2025**, *27*, 15124–15134. [CrossRef]
13. Vozniak, A.; Hosseinnezhad, R.; Vozniak, I.; Galeski, A. PET Mechanical Recycling. A New Principle for Chain Extender Introduction. *Sustain. Mater. Technol.* **2024**, *40*, e00886. [CrossRef]
14. Valenzuela-Ortega, M.; Suitor, J.T.; White, M.F.M.; Hinchcliffe, T.; Wallace, S. Microbial Upcycling of Waste PET to Adipic Acid. *ACS Cent. Sci.* **2023**, *9*, 2057–2063. [CrossRef] [PubMed]
15. Podara, C.; Termine, S.; Modestou, M.; Semitekolos, D.; Tsirogiannis, C.; Karamitrou, M.; Trompeta, A.-F.; Milickovic, T.K.; Charitidis, C. Recent Trends of Recycling and Upcycling of Polymers and Composites: A Comprehensive Review. *Recycling* **2024**, *9*, 37. [CrossRef]
16. Fiorillo, C.; Trossaert, L.; Bezeraj, E.; Debrie, S.; Ohnmacht, H.; Van Steenberge, P.H.M.; D'hooge, D.R.; Edeleva, M. Molecular and Material Property Variations during the Ideal Degradation and Mechanical Recycling of PET. *RSC Sustain.* **2024**, *2*, 3596–3637. [CrossRef]
17. Schyns, Z.O.G.; Patel, A.D.; Shaver, M.P. Understanding Poly(Ethylene Terephthalate) Degradation Using Gas-Mediated Simulated Recycling. *Resour. Conserv. Recycl.* **2023**, *198*, 107170. [CrossRef]
18. Chamas, A.; Moon, H.; Zheng, J.; Qiu, Y.; Tabassum, T.; Jang, J.H.; Abu-Omar, M.; Scott, S.L.; Suh, S. Degradation Rates of Plastics in the Environment. *ACS Sustain. Chem. Eng.* **2020**, *8*, 3494–3511. [CrossRef]
19. Yang, T.; Yang, Z.; Zhang, Y.; Hu, C.; Xie, Z.; Sun, Z.; Pang, X.; Chen, X. Upcycling of PET Waste: From One Polymer to Another Polymer. *Polym. Chem.* **2026**, *17*, 7–20. [CrossRef]
20. Alzahrani, M.; Alhumade, H.; Simon, L.; Yetilmezsoy, K.; Madhuranthakam, C.M.R.; Elkamel, A. Additive Manufacture of Recycled Poly(Ethylene Terephthalate) Using Pyromellitic Dianhydride Targeted for FDM 3D-Printing Applications. *Sustainability* **2023**, *15*, 5004. [CrossRef]
21. Karl, C.W.; Arstad, B.; Shamsuyeva, M.; Lecinski, J.; Olafsen, K.; Larsen, Å.G.; Kubowicz, S.; Comerford, J.; Endres, H.-J. Upgrading and Enhancement of Recycled Polyethylene Terephthalate with Chain Extenders: In-Depth Material Characterization. *Ind. Eng. Chem. Res.* **2024**, *63*, 12277–12287. [CrossRef]
22. Standau, T.; Nofar, M.; Dörr, D.; Ruckdäschel, H.; Altstädt, V. A Review on Multifunctional Epoxy-Based Joncryl® ADR Chain Extended Thermoplastics. *Polym. Rev.* **2022**, *62*, 296–350. [CrossRef]
23. Truscello, A.; Colletti, S.; Gambarotti, C.; Ortenzi, M.A.; Gazzotti, S.; Galimberti, M.S. Biosourced Aromatic Derivatives in the Upcycling of Recycled PET: Mellophanic Dianhydride as a Chain Extender. *ACS Sustain. Chem. Eng.* **2023**, *11*, 9721–9728. [CrossRef]
24. Mestry, J.; Abdelwahab, M.A.; Elkholy, H.M.; Rabnawaz, M. Superior Glycidol-Free Chain Extenders for Post-Consumer PET Bottles and PET Thermoform Blends. *Resour. Conserv. Recycl.* **2024**, *203*, 107420. [CrossRef]
25. van der Maas, K.; Weinland, D.H.; van Putten, R.-J.; Wang, B.; Gruter, G.-J.M. Catalyst Free PET and PEF Polyesters Using a New Traceless Oxalate Chain Extender. *Green. Chem.* **2024**, *26*, 11182–11195. [CrossRef]
26. Bustos Seibert, M.; Mazzei Capote, G.A.; Gruber, M.; Volk, W.; Osswald, T.A. Manufacturing of a PET Filament from Recycled Material for Material Extrusion (MEX). *Recycling* **2022**, *7*, 69. [CrossRef]
27. Aly, R.; Vijay, S.; Shyju, V.; Sharfuddin, M.; Samad, W.A. Recycling Plastic Water Bottles into High Quality Filaments for Sustainable 3D Printing. *Discov. Mech. Eng.* **2025**, *4*, 71. [CrossRef]
28. Rashwan, O.; Koroneos, Z.; Townsend, T.G.; Caputo, M.P.; Bylone, R.J.; Wodrig, B.; Cantor, K. Extrusion and Characterization of Recycled Polyethylene Terephthalate (RPET) Filaments Compounded with Chain Extender and Impact Modifiers for Material-Extrusion Additive Manufacturing. *Sci. Rep.* **2023**, *13*, 16041. [CrossRef] [PubMed]
29. Siriorn, I.N.A.; Munchumart, B.; Natanicha, B.; Nut, S.; Nopparat, M.; Suchart, H. Viscosity Improvement of Recycled Poly (Ethylene Terephthalate) from Waste Bottles by Adding Antioxidants and Chain-Extender. *E3S Web Conf.* **2021**, *302*, 02019. [CrossRef]
30. Guclu, M.; Alkan Göksu, Y.; Özdemir, B.; Ghanbari, A.; Nofar, M. Thermal Stabilization of Recycled PET Through Chain Extension and Blending with PBT. *J. Polym. Environ.* **2022**, *30*, 719–727. [CrossRef]
31. Arayesh, H.; Golshan Ebrahimi, N.; Khaledi, B.; Khabazian Esfahani, M. Introducing Four Different Branch Structures in PET by Reactive Processing—A Rheological Investigation. *J. Appl. Polym. Sci.* **2020**, *137*, 49243. [CrossRef]

32. Scheirs, J. Additives for the Modification of Poly(Ethylene Terephthalate) to Produce Engineering-Grade Polymers. In *Modern Polyesters: Chemistry and Technology of Polyesters and Copolyesters*; Wiley: Hoboken, NJ, USA, 2004; pp. 495–540.
33. Cusano, I.; Campagnolo, L.; Costanzo, S.; Aurilia, M.; Grizzuti, N. Enhancement of Polyethylene Terephthalate Rheological Properties via Chain Extension and Branching: A Design of Experiment Approach. *Adv. Mater. Sci. Eng.* **2026**, *2026*, 3358838. [CrossRef]
34. Incarnato, L.; Scarfato, P.; Di Maio, L.; Acierno, D. Structure and Rheology of Recycled PET Modified by Reactive Extrusion. *Polymer* **2000**, *41*, 6825–6831. [CrossRef]
35. Candal, M.V.; Safari, M.; Fernández, M.; Otaegi, I.; Múgica, A.; Zubitur, M.; Gerrica-echevarria, G.; Sebastián, V.; Irusta, S.; Loaeza, D.; et al. Structure and Properties of Reactively Extruded Opaque Post-Consumer Recycled PET. *Polymers* **2021**, *13*, 3531. [CrossRef] [PubMed]
36. Härth, M.; Dörnhöfer, A. Film Blowing of Linear and Long-Chain Branched Poly(Ethylene Terephthalate). *Polymers* **2020**, *12*, 1605. [CrossRef] [PubMed]
37. *ISO 527-2*; Plastics—Determination of Tensile Properties—Part 2: Test Conditions for Moulding and Extrusion Plastics. International Organization for Standardization: Geneva, Switzerland, 2012.
38. *ISO 291*; Plastics—Standard Atmospheres for Conditioning and Testing. International Organization for Standardization: Geneva, Switzerland, 2008.
39. Dalsin, S.J.; Hillmyer, M.A.; Bates, F.S. Molecular Weight Dependence of Zero-Shear Viscosity in Atactic Polypropylene Bottlebrush Polymers. *ACS Macro Lett.* **2014**, *3*, 423–427. [CrossRef]
40. Kader, S.; Akdevelioğlu, Y.; Özdemir, B.; Nofar, M. *How the Molecular Weight of a Polyester Could Influence the Reactivity of Joncryl Chain Extender?* AIP Publishing LLC: Melville, NY, USA, 2023; p. 160001.
41. Dörr, D.; Standau, T.; Murillo Castellón, S.; Bonten, C.; Altstädt, V. Rheology in the Presence of Carbon Dioxide (CO_2) to Study the Melt Behavior of Chemically Modified Polylactide (PLA). *Polymers* **2020**, *12*, 1108. [CrossRef]
42. Eslami, H.; Kamal, M.R. Effect of a Chain Extender on the Rheological and Mechanical Properties of Biodegradable Poly(Lactic Acid)/Poly[(Butylene Succinate)-*Co*-adipate] Blends. *J. Appl. Polym. Sci.* **2013**, *129*, 2418–2428. [CrossRef]
43. Erdmann, R.; Rennert, M.; Meins, T. Influence of Epoxy Functional Chain-Extenders on the Thermal and Rheological Properties of Bio-Based Polyamide 10.10. *Polymers* **2023**, *15*, 3571. [CrossRef]
44. Altınbay, A.; Özsaltık, C.; Jahani, D.; Nofar, M. Reactivity of Joncryl Chain Extender in PLA/PBAT Blends: Effects of Processing Temperature and PBAT Aging on Blend Performance. *Int. J. Biol. Macromol.* **2025**, *303*, 140703. [CrossRef]
45. Šudomová, L.; Doležalová Weissmannová, H.; Steinmetz, Z.; Řezáčová, V.; Kučeřík, J. A Differential Scanning Calorimetry (DSC) Approach for Assessing the Quality of Polyethylene Terephthalate (PET) Waste for Physical Recycling: A Proof-of-Concept Study. *J. Therm. Anal. Calorim.* **2023**, *148*, 10843–10855. [CrossRef]
46. Gomes, S.; Pimentel, A.; Monteiro, M.J.; Marinho, A.; Melo, A. Thermal and Chemical Characterisation of Reprocessed PET: A Study on Commercial, Recycled, Bottle-Grade and Textile Blend. *Materials* **2025**, *18*, 4394. [CrossRef] [PubMed]
47. Aliberti, F.; Oliviero, M.; Longo, R.; Guadagno, L.; Sorrentino, A. Effect of Crystallinity on the Printability of Poly(Ethylene Terephthalate)/Poly(Butylene Terephthalate) Blends. *Polymers* **2025**, *17*, 156. [CrossRef]
48. Straková, M.; Hlaváčiková, S.; Feranc, J.; Suchánková, H.; Kramárová, Z.; Ďurfina, M.; Omaníková, L.; Hezaveh, M.R.; Tomanová, K.; Vanovčanová, Z.; et al. Effects of Repeated Thermo-Mechanical Processing on the Degradation Behavior of Bottle-Grade PET Under Controlled Conditions. *Polymers* **2026**, *18*, 416. [CrossRef]
49. Odet, F.; Ylla, N.; Delage, K.; Cassagnau, P. Influence of Chain Extenders on Recycled Standard and Opaque PET Rheology and Melt-Spun Filament Properties. *ACS Appl. Polym. Mater.* **2022**, *4*, 8290–8302. [CrossRef]
50. Zhao, Z.; Wu, Y.; Wang, K.; Xia, Y.; Gao, H.; Luo, K.; Cao, Z.; Qi, J. Effect of the Trifunctional Chain Extender on Intrinsic Viscosity, Crystallization Behavior, and Mechanical Properties of Poly(Ethylene Terephthalate). *ACS Omega* **2020**, *5*, 19247–19254. [CrossRef]
51. Di Lorenzo, M.L. Crystallization of Poly(Ethylene Terephthalate): A Review. *Polymers* **2024**, *16*, 1975. [CrossRef]
52. Heinze, D.A.; Das, A.; Williams, C.B.; McIlroy, C.; Peterson, A.M.; Bortner, M.J. Realizing Semicrystalline Polymer Physics across Disparate Processing Scales: From Desktop Extrusion to Large-Format Additive Manufacturing. *Prog. Polym. Sci.* **2026**, *172*, 102053. [CrossRef]

Disclaimer/Publisher's Note: The statements, opinions and data contained in all publications are solely those of the individual author(s) and contributor(s) and not of MDPI and/or the editor(s). MDPI and/or the editor(s) disclaim responsibility for any injury to people or property resulting from any ideas, methods, instructions or products referred to in the content.